

### **43<sup>rd</sup> Biennial Meeting of the German Colloid Society**

This volume contains selected papers presented at the 43<sup>rd</sup> Biennial Meeting of the German Colloid Society held at the Schloß Waldthausen near Mainz, October 8–10, 2007. The meeting's emphasis was given to "Surface and Interfacial Forces – From Fundamentals to Applications" but also provided a general overview on current aspects of colloid and polymer science in fundamental research and applications.

The contributions in this volume are representative of the richness of research topics in colloid and polymer science. They cover a broad field including the application of scanning probe techniques to colloid and interface science, surface induced ordering, novel developments in amphiphilic systems as well as the synthesis and applications of nano-colloids.

The meeting brought together people from different fields of colloid, polymer, and materials science and provided the platform for dialogue between scientists from universities, industry, and research institutions.

Günter K. Auernhammer  
Hans-Jürgen Butt  
Doris Vollmer

M. Maas  
H. Rehage  
H. Nebel  
M. Eppele

## Formation and Structure of Coherent, Ultra-thin Calcium Carbonate Films below Monolayers of Stearic Acid at the Oil/Water Interface

**Abstract** Detailed investigations of interfacial crystallization procedures are important to understand the basic principles of biomineralization processes. These interfacial phenomena can also be used to form new types of biomimetic composite materials. In a series of experiments we studied the influence of Langmuir-monolayers on the formation of ultra-thin calcium carbonate films. We systematically compared experiments performed at the water surface with results obtained at the water/oil interface. For stearic acid monolayers formed at the pure water surface, we were able to observe densely packed dispersions of ultra-thin  $\text{CaCO}_3$  crystals, which were adsorbed below

the surfactant membranes. We analyzed details of these structures by means of Brewster-angle-microscopy and other microscopic techniques. At the oil/water interface, however, we observed the formation of coherent, ultra-thin calcium carbonate films. These extended, two-dimensional crystalline structures were characterized by scanning electron microscopy, X-ray diffraction, and other techniques like interfacial-shear-rheology.

**Keywords** Biomineralization · Calcium carbonate · Stearic acid · Thin film · Amorphous precursor · Monolayer · Interface

M. Maas (✉) · H. Rehage  
Chair of Physical Chemistry II, Technical  
University of Dortmund, 44227 Dortmund,  
Germany  
e-mail: michael.maas@uni-dortmund.de

H. Nebel · M. Eppele  
Institute of Inorganic Chemistry, University  
of Duisburg-Essen, 45117 Essen, Germany

### Introduction

Biomineralization is a natural process that ultimately leads to the formation of complex nano-structured materials. These special structures are assembled by highly controlled growth mechanisms at the organic/inorganic interface [1–5]. Extensive research in the field of biomineralization is not only important for the comprehension of the processes in nature but could also lead to the development of advanced techniques for the architecture of new materials.

Calcium carbonate is the most important biomineral, due to its presence in, e.g., mollusk shells, skeletons of foraminiferes, coccolithophores, or corals (see [6] for a recent review).

A straightforward attempt that can be used to study biomineral growth is based on the application of Lang-

muir films. These lipid monolayers provide a simple model system for the organic/inorganic interface present in biomineralization, e.g., membranes or protein surfaces. In most of our experiments we studied stearic acid monolayers that were spread on a calcium hydrogencarbonate ( $\text{Ca}(\text{HCO}_3)_2$ ) subphase [7]. These films were studied by Brewster angle microscopy (BAM), scanning-electron-microscopy (SEM), and other techniques.

The air/water interface in combination with Langmuir films of lipids or fatty acids is generally considered as a good modeling system for biomineralization processes occurring in cells or vesicles. In nature, of course, the mineralization takes place within the organisms without contact to air. So our approach was to transfer the experiments we first performed at the air/water interface to the oil/water interface. This, again, is a simplification compared to the bilayer membranes of cells that separate

two aqueous phases. The results that we observed at the oil/water interface were completely different from what we measured at the air/water surface. In the latter studies only transient precursor films were observed, which turned into isolated crystals after a short period of time. At the oil/water interface, however, closed, durable films formed spontaneously within 12 h. Solid films of calcium carbonate composite materials were already prepared by other groups with additives such as polyelectrolytes [8–19] (mainly polyacrylic acid (PAA)) or high ratios of magnesium salts [20–22]. The additives serve as crystallization inhibitors in the bulk phase and tend to stabilize the  $\text{CaCO}_3$  amorphous precursor phase in proximity to the interface. After addition of these compounds, macroscopic films with micrometer to nanometer thickness were obtained. In our experiments we observed the formation of stable films without adding crystallization inhibitors. The shear rheological properties of these films were measured with a custom built 2d-Couette system in order that the growth time and the stability of the films were evaluated. The interpretation of the rheological data also allows suggestions about the composition and structure of the films. Further, scanning electron micrographs and X-ray powder diffraction analysis are provided for a more detailed characterization. In this publication we focus on a brief overview of our work and compare the two strategies of biomineralization studies.

## Materials and Methods

### Substances

All substances were purchased at analytical grade from VWR company and used without further purification. Millipore grade water was prepared by an Elsa Purelab Ultra at 18.2 M $\Omega$ .

### Preparation of the $\text{Ca}(\text{HCO}_3)_2$ Solutions

For the preparation of the  $\text{Ca}(\text{HCO}_3)_2$  solutions several grams of  $\text{CaCO}_3$  were suspended in 0.5 L water and flushed with gaseous  $\text{CO}_2$  for about 2 h. In order to remove excess  $\text{CaCO}_3$  the solution was filtered. In addition, the solutions were filtered again before each application. The concentration of the  $\text{Ca}(\text{HCO}_3)_2$  solutions prepared by this method was approximately 8 mM (determined by titration with EDTA). The pH of this solution was 7.2.

### Experiments at the Air/Water Interface

**BAM Experiments.** For all experiments a Langmuir–Blodgett trough (NIMA-Technology, Coventry, England, Type 601 BAM) was filled with 200 mL of water (Elsa Purelab Ultra, 18.2 M $\Omega$ ). Afterwards, stearic acid solution was spread at the water surface. After evaporation of the

solvent chloroform (about 5 min) the lipid monolayer was compressed until a solid-condensed film occurred with  $\Pi_0$  (surface pressure)  $\approx 25 \text{ mN m}^{-1}$ . In order to generate well-defined domain structures, the solid condensed film was expanded and compressed several times. Afterwards, the 8 mM solution of  $\text{Ca}(\text{HCO}_3)_2$  was induced into the subphase by means of a perfusor pump, and the excess water was simultaneously removed in order to obtain a constant water level. The induction speed was  $25 \text{ mL h}^{-1}$ , so that a homogeneous distribution of the ions in the subphase was reached by diffusion. This distribution was created in order to ensure a controlled monitoring of the crystallization processes. Experiments at which the stearic acid was directly spread onto the subphase were performed as well, but there it was difficult to observe the first crystallization steps. Overall the results of these simpler experiments were equivalent to the infusion technique. During these experiments, the water surface was monitored by Brewster angle microscopy.

**Scanning Electron Microscopy.** For scanning electron microscopy 150  $\mu\text{L}$  stearic acid (1 mM) was spread onto 400 mL of a 6 mM  $\text{Ca}(\text{HCO}_3)_2$  solution in a Langmuir–Blodgett trough. The films were compressed to surface pressures of about  $30 \text{ mN m}^{-1}$ . At a specified time after the surface pressure was obtained (app. 30 min after the beginning of the experiment), the films were transferred by the same technique as described in the above paragraph. Remaining water droplets were quickly removed from the surface. A silicon wafer was applied as substrate, which was made hydrophobic. For this purpose silicon wafers were aligned next to a drop of dimethyldichlorosilane, left in an exsiccator over night and, afterwards, were washed with freshly distilled acetone. Different samples were prepared at temperatures between 5 and 40 °C. At 20 °C additional samples were prepared at different  $\text{Ca}(\text{HCO}_3)_2$  concentrations. The growth time and the pH were varied. These samples were investigated by a FEI ESEM Quanta 400 scanning electron microscope that was equipped with energy-dispersive X-ray spectroscopy (EDAX EDS Genesis 4000).

### Experiments at the Oil/Water Interface

**General Experiment.** 50 mL of the freshly filtered  $\text{Ca}(\text{HCO}_3)_2$  solution was put into a 100 mL crystallization dish (diameter 70 mm, height 40 mm). 40 mL of a 1 mM solution of stearic acid, in either dodecane or toluene, was added to the original solution. Samples for SEM or XRD were taken after specific amounts of time. Control experiments were carried out by exchanging the aqueous phase with 4 mM  $\text{Na}(\text{HCO}_3)_2$ , 4 mM  $\text{CaCl}_2$ , and pure water while maintaining the organic phase (and exchanging the stearic acid with different lipids, while maintaining the aqueous phase). No films were obtained under these conditions.

**Scanning Electron Microscopy.** For scanning electron microscopy at a specified time after the start of the experiments, a silicon wafer was quickly dipped with the sharp edge through the film and carefully pulled out again in a way that the lower side of the film was attached to the surface of the wafer. Samples were prepared at different  $\text{Ca}(\text{HCO}_3)_2$  concentrations and different growth times at room temperature. These samples were investigated by a FEI ESEM Quanta 400 scanning electron microscope which was equipped with energy-dispersive X-ray spectroscopy (EDAX EDS Genesis 4000).

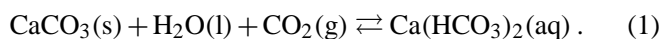
**X-ray Powder Diffractometry.** The material was obtained by collecting film fragments out of the crystallization dishes with a spatula and then studied in transmission mode on a Kapton foil with a Siemens D5000 diffractometer using  $\text{Cu K}_\alpha$  radiation ( $\lambda = 1.54 \text{ \AA}$ ). Additionally, one sample was measured with pure  $\text{CaCO}_3$  powder and stearic acid (the same as used for the preparation of the samples).

**Rheology.** The shear rheological properties of the films were determined by a Rheometrics fluid spectrometer (RFS II), which was equipped with a modified shear system [23]. The measuring cell consisted of a quartz dish (diameter 83.6 mm) and a thin biconical titanium plate (angle  $2^\circ$ , diameter 60 mm), which were placed exactly at the interface between oil and water. The dish was first filled with the aqueous phase (100 mL). The titanium plate was then positioned at the water surface and the stearic acid solution was added (40 mL). We measured the torque required to hold the plate stationary as the cylindrical dish was rotated with the sinusoidal angular frequency  $\omega$ . In such experiments, the two-dimensional storage modulus  $\mu'(\omega)$  and the loss modulus  $\mu''(\omega)$  were evaluated from the amplitude and phase angle of the stress and deformation signals.

## Results and Discussion

### Crystallization at the Air/Water Interface

In analogy to experiments performed by Hacke [24, 25], we investigated the crystallization of  $\text{CaCO}_3$  under a monolayer of stearic acid. For a more detailed presentation of these results see [7]. If stearic acid is quickly spread onto an aqueous subphase of calcium hydrogencarbonate, thin films of  $\text{CaCO}_3$  emerge in direct proximity to the Langmuir film. In the aqueous subphase the following equilibrium reaction occurs:



This reaction also takes place during natural mineralization processes. Therefore, this simple membrane system is well suited to model biomineralization.

In the following, only these phenomena that are linked to the formation of thin films or precursor aggregates are shown. In almost all cases, a large amount of calcite single crystals appeared sooner or later together with those structures and eventually sedimentate towards the ground of the reaction vessel. The formation of such calcite crystals is well documented in the literature [26–31] and shall only be discussed here if they contribute to understanding the observed processes.

X-ray diffraction analysis of the films showed calcite, vaterite, and a broad amorphous region due to the organic material and/or amorphous calcium carbonate.

### Brewster-Angle-Microscopy

The thin  $\text{CaCO}_3$  film which was formed under the Langmuir monolayer of stearic acid could easily be investigated by means of BAM. A typical BAM-image of such a film is shown in Fig. 1.

In a series of different experiments, we observed the formation of transient films only under densely packed monolayers of stearic acid ( $\Gamma = 25 \text{ mN/m}$ ). In a typical experiment, 50 mL of an 8 mM aqueous solution of  $\text{Ca}(\text{HCO}_3)_2$  were introduced into the subphase during two hours (starting concentration: 0 mM, final concentration: 2 mM). Immediately after the beginning of the experiment, first particles with a diameter of around 200 nm (the maximum lateral resolution) formed at defects of the monolayer. These defects appeared as bright dots that were present already before the  $\text{Ca}(\text{HCO}_3)_2$  solution was induced. The calcium carbonate particles appeared as white dots and could only be differentiated by extensive blank tests with pure water or calcium chloride as subphase. Consecutively these particles started to form fractal aggregates. With increasing time (accordingly increasing the  $\text{Ca}(\text{HCO}_3)_2$  concentration), the aggregates became more densely packed, until finally a thin closed film was present. Note that it was difficult to derive the size of the particles from these experiments. The maximum lateral resolution of BAM is of the order of  $0.2 \text{ }\mu\text{m}$ , therefore the occurrence of larger and smaller particles at the same time leads to a superposition of particles that can be regularly depicted and those which are smaller than the resolution of the microscope. The latter are observed as Newtonian rings. Therefore, the fine structure in Fig. 1 can be misleading.

### Scanning Electron Microscopy

A more detailed inspection of the observed structures was made possible by means of scanning electron microscopy (SEM). The selected images provide a close look onto the crystal shapes and surfaces. However, it is more difficult to get information by SEM about the height or the thickness of the films. The structures observed here can be compared to those described above. Generally, the dark, plane regions represent the lipid monolayer with the head groups



**Fig. 1** Thin film of  $\text{CaCO}_3$  below a stearic acid monolayer ( $\Gamma_0 = 25 \text{ mN m}^{-1}$ ,  $T = 22 \text{ }^\circ\text{C}$ ,  $\text{pH} = 7$ )

facing towards the observer. As reported earlier [32–35] calcite and vaterite crystals were observed, depending on the experimental conditions. Here attention was drawn to the more irregular, yet reproducible structures. All of the presented objects consisted of calcium carbonate as verified by quantitative EDX analysis and were rather seldomly observed but were reproducible. At  $20 \text{ }^\circ\text{C}$  we observed large, layered structures in the vicinity of single crystals. A closer inspection of the surface of these objects revealed that these structures consisted of calcium carbonate aggregates, composed of small particles with a diameter of about 30–60 nm. The reason that only a few of these objects can be observed could be that they are metastable. Over time, they may develop into branched vaterite crystals, or they are forming clusters grown out calcite or vaterite crystals. This is concluded by comparison of the structures from BAM and SEM, as it is impossible

to observe phase transitions under these conditions (in the given time frame) due to the lack of water.

At a lower temperature of  $5 \text{ }^\circ\text{C}$ , a large number of leaf-like structures was observed. Again these objects consisted of smaller particles that typically had diameters between 50 and 100 nm. Similar structures were observed at very low subphase concentrations (see Fig. 2). The structures on the lower side of the lower “leaf” shown in Fig. 2 resemble small vaterite florets in an early growth state. So it may be assumed that these objects are metastable intermediates or precursor-aggregates that are trapped in this state because of the removal of water. The size of the particles from which these structures were formed was about 50–100 nm. From these observations it can also be concluded that the primary calcium carbonate particles are more stable at lower temperatures or very low subphase concentrations.

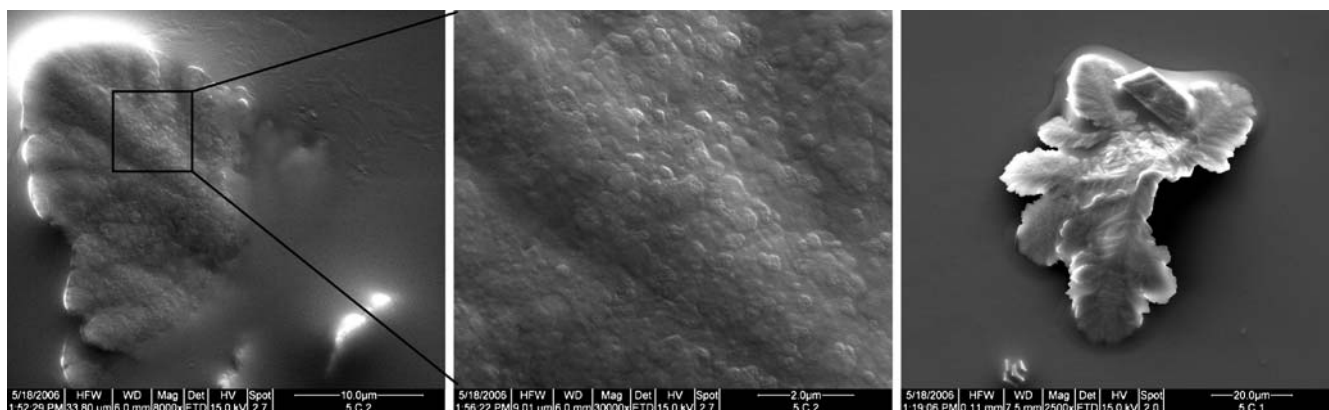


**Fig. 2** Typical SEM-Images of leaf-like calcium carbonate films formed below a monolayer of stearic acid at  $T = 5 \text{ }^\circ\text{C}$ ,  $[\text{Ca}(\text{HCO}_3)_2] = 6 \text{ mM}$ ,  $t_{\text{growth}} = 1.5 \text{ h}$ ,  $\Gamma_0 = 30 \text{ mN m}^{-1}$ ,  $\text{pH} = 7$ . The films consisted of small particles with typical diameters between 50 and 100 nm

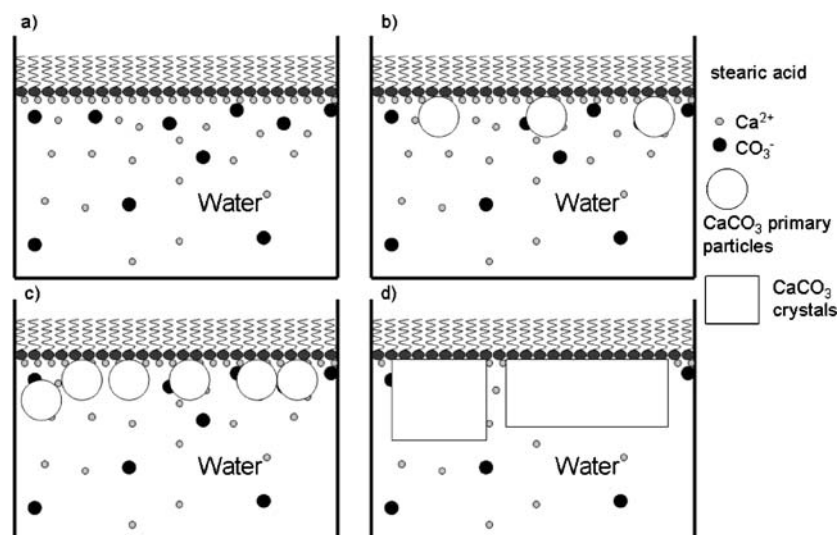
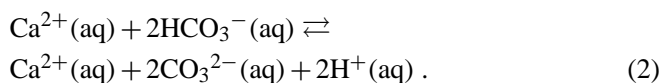


**Fig. 3** Schematic picture of the formation of a  $\text{CaCO}_3$  thin film under a monolayer of stearic acid

Under these assumptions these structures can be explained by mechanisms of colloidal growth processes. In other words, a self-organization process on the mesoscale through the assembly of calcium carbonate nanoparticles is assumed [36]. The polymorphic phase of these primary particles could not be determined in these experiments due to the small amount of substance available.

## Conclusion

There are still some basic questions unresolved regarding the aggregation processes of  $\text{CaCO}_3$  primary particles. As the particles have a net negative surface charge [37], adsorption and aggregation processes to the negatively charged stearic acid film appear to be energetically unfavorable. Here, the accumulation of the particles in proximity to the monolayer can only be induced by the compensation of the negative charges at the particle surfaces. This can be achieved by positively charged counter ions that adsorb on the surface of the nanoparticles. In monolayers of fatty acids protons can be supplied by the carboxylic head groups and cations from the subphase can be accumulated. Thus, the surface charge of the particles can be reduced or compensated so that the particles become able to adsorb at the monolayer. Concerning the formation of  $\text{CaCO}_3$  crystals, another electrostatic effect has to be taken into account. The importance of this effect becomes clear by considering the following reaction:



If the proton concentration is increased, the equilibrium shown in this equation shifts to the left. That means that the formation of  $\text{CaCO}_3$  crystals is disfavored. It

may be possible that this also means that the stability of the primary particles, which were formed before grown out  $\text{CaCO}_3$  crystals occurred [38, 39], increases. Note that only the proton concentration in proximity to the head groups of the lipids is concerned. If the bulk pH is altered the crystallization is no longer controlled by the interface. The observed formation of the  $\text{CaCO}_3$  thin films can be described as presented in Fig. 3: Below the stearic acid monolayer, a supersaturation of calcium and hydrogencarbonate ions occurred (Fig. 3a). From this supersaturated phase in proximity to the Langmuir film calcium carbonate particles formed (Fig. 3b). If the primary particles remained stable for a longer period of time, the particles could aggregate (Figure 3c) and form a thin film. This precursor film finally converted into more stable  $\text{CaCO}_3$  modifications, like leaf-like structures, vaterite-flower-crystals, or clusters of well-developed calcite crystals and vaterite crystal agglomerations (Fig. 3d).

## Crystallization at the Oil/Water Interface

After a growth time of 12 h, the films were visible to the unaided eye. They appeared as a translucent, slightly glossy membrane at the oil/water interface. After drying, the films appeared white with a crystalline glimmer. The drying of the films often led to breaking and sometimes to furling, probably due to different features of the upper and lower side. Derived from the experimental setup, the upper side of the films is the side that was exposed to the organic phase and the lower side the one exposed to the aqueous phase. Table 1 summarizes the different experiments. X-ray diffraction analysis of the films showed calcite, stearic acid, calcium stearate, and traces of vaterite.

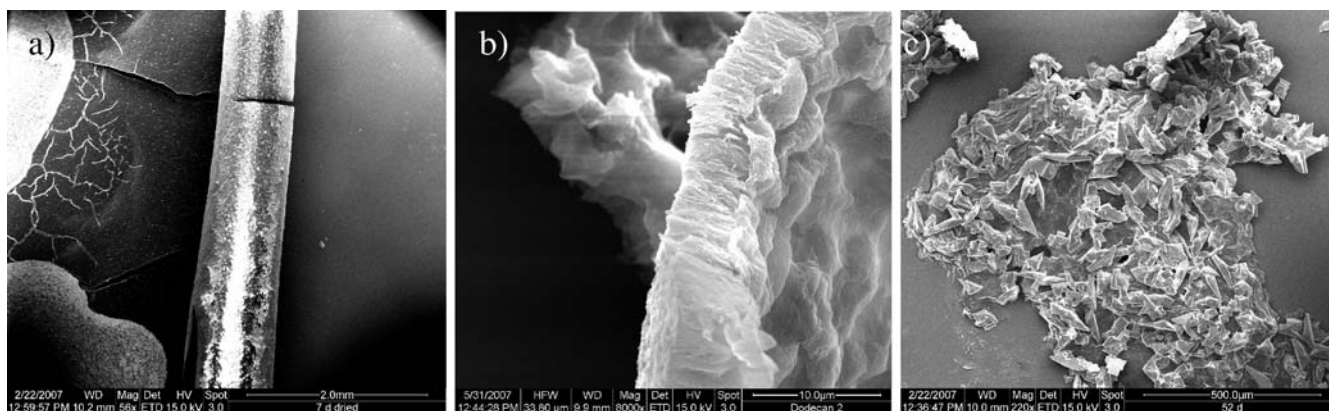


**Fig. 4** 4 mM  $\text{Ca}(\text{HCO}_3)_2$ , 1 mM stearic acid in toluene, growth time 7 days. **a** Upper side with furled section; **b** Side view; **c** 4 mM  $\text{Ca}(\text{HCO}_3)_2$ , 1 mM stearic acid in toluene, growth time 52 days

**Table 1** Summary of experiments

Organic phase	Aqueous phase	Film formation
1 mM stearic acid in toluene	4 mM $\text{Ca}(\text{HCO}_3)_2$	Yes
Toluene	4 mM $\text{Ca}(\text{HCO}_3)_2$	No
1 mM stearic acid in toluene	Water	No
1 mM stearic acid in toluene	4 mM $\text{Na}(\text{HCO}_3)$	No
1 mM stearic acid in toluene	4 mM $\text{CaCl}_2$	No

### Scanning Electron Microscopy

SEM provides a close look at dried versions of the films. Figure 4a depicts a large fragment of a film that furled on the right side so that the lower side became visible. Note the difference in roughness between both sides. Figure 4b allowed the estimation of the film thickness, which was roughly about 10  $\mu\text{m}$  after 7 days of growth.

Figure 4c shows a film that was left in the reaction vessel for one and a half months. In contrast to the films that grew over one week, here, crystalline shapes were observed as components of the membrane. Due to the rectangular shapes of these crystals and compared to the XRD analysis they were mainly deformed calcite crystals.

### 2d-Shear-Rheology

At constant deformation and frequency, the two-dimensional viscoelastic properties of the films were measured as a function of time. With this kind of experiment the growth of the films was monitored. In case of the toluene films (Fig. 6a), 12–24 h after the beginning of the experiments, an elastic film formed. After the initial growth, the moduli decreased again, and the distance between storage and loss module increased in favor of the storage module. The local minimum and the increase in elasticity were probably due to crystallization processes inside the films. After approximately three days the moduli remained stable

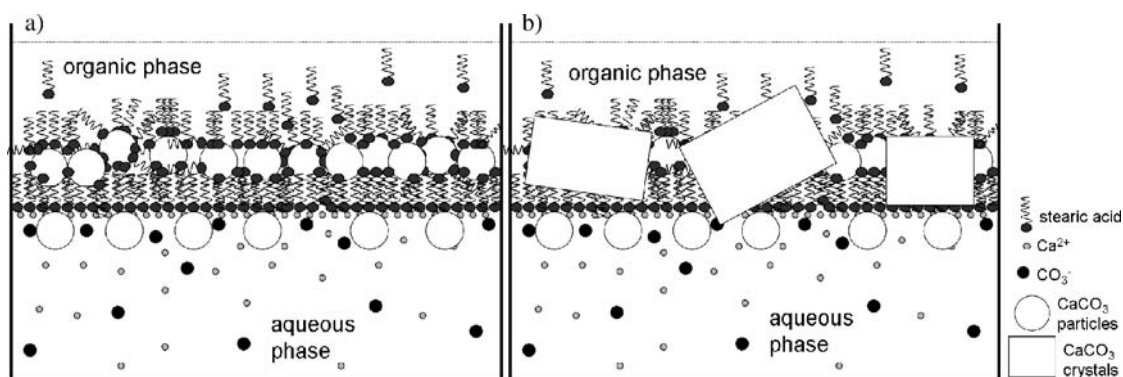


**Fig. 5** Simplified model of the formation of the thin films: **a** Aggregation of precrystalline calcium carbonate particles at the oil/water interface, **b** Crystallization of the precrystalline calcium carbonate

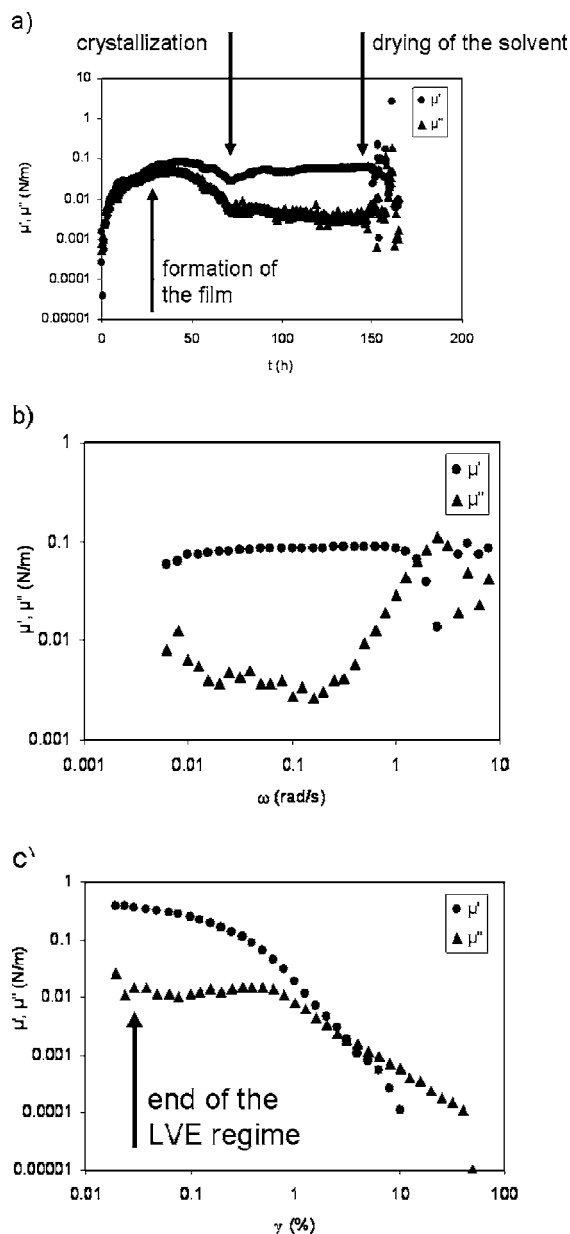


**Fig. 6** **a** Time ( $\gamma = 0.2\%$ ,  $\omega = 0.0016$  Hz), **b** frequency ( $\gamma = 0.1\%$ ) and **c** deformation ( $\omega = 0.016$  Hz) tests for 4 mM  $\text{Ca}(\text{HCO}_3)_2$ , 1 mM stearic acid in toluene. The frequency test was performed after three days of growth time, the deformation test after 4 days

until the toluene was evaporated. The reason for the overall values of the moduli being very small was due to the smaller thickness of the films.

If the films were sufficiently stable (after 3 days) it was possible to measure  $\mu'$  and  $\mu''$  at very low frequencies (Fig. 6b). Such measurements typically last from four to eight hours. As a result of these experiments, it can be concluded that the films behaved like viscoelastic, solid materials. This is because the moduli were parallel over the whole frequency spectrum with the storage modulus being the higher one. As an exception to this, the loss modulus increased at very high angular velocities because of the glass-analogous behavior of the films.

The brittleness and crystalline character of the films was emphasized by the deformation test. The linear viscoelastic regime (the deformation range at Fig. 6c which the films are deformed reversibly) was limited to deformations of about 0.1%, which is an extremely low value. This points to the presence of energy elastic systems. As a compromise to the resolution of the measuring device, in the other test setups the applied strain was set to 0.1 or 0.2%.

## Conclusion

From the experimental data it can be concluded that the films have a diameter of about 5–10  $\mu\text{m}$  and consisted of stearic acid, calcium stearate, and calcium carbonate (mainly calcite, no experimental information could be given concerning amorphous calcium carbonate at this point). The viscoelastic data pointed to a glassy state with a crystalline hardness. It is important to note that the films did not consist of a stearate monolayer, cross-linked by calcium ions (chalk soaps) as control experiments with  $\text{CaCl}_2$  observed. Derived from other control experiments it became clear that the growth of the films was due to a specific interaction of crystalline (or precrystalline) calcium carbonate and stearic acid.

In analogy to the studies at the air/water interface we suggest a growth mechanism involving calcium carbonate nanoparticles, which served as precursor particles. Osmotic draining of locally constrained emulsion droplets could also lead to crystallization processes. Further experiments shall involve high resolution X-ray diffraction and FTIR studies in order to evaluate the role of amorphous calcium carbonate in the crystallization processes.

---

**References**

1. Baeuerlein E (2000) *Biom mineralization*. Wiley-VCH, Weinheim
2. Baeuerlein E (2003) *Angew Chem Int Edn* 42:614–641
3. Baeuerlein E (2004) *Biom mineralization. Progress in Biology, Molecular Biology and Application*. Wiley-VCH, Weinheim, New York
4. Lowenstam HA, Weiner S (1989) *On biom mineralization*. Oxford University Press, New York
5. Mann S (2001) *Biom mineralization; principles and concepts in bioinorganic materials chemistry*. Oxford University Press, Oxford
6. Meldrum FC (2003) *Int Mater Rev* 48:187–224
7. Maas M, Rehage H, Nebel H, Epple M (2007) *Colloid Polym Sci* 285:1301–1311
8. Yu S-H, Cölfen H (2004) *J Mater Chem* 14:2124–2147
9. Cölfen H, Mann S (2003) *Adv Mater Int Edit* 42:2350–2365
10. Xu G, Aksay IA, Groves JT (2001) *J Am Chem Soc* 123:2196–2203
11. Xu X, Han JT, Cho K (2004) *Chem Mater* 16:1740–1746
12. DiMasi E, Patel VM, Sivakumar M, Olszta MJ, Yang YP, Gower LB (2002) *Langmuir* 18:8902–8909
13. Volkmer D, Harms M, Gower L, Ziegler A (2005) *Adv Mater Int Edit* 44:639–644
14. Xu G, Yao N, Aksay IA, Groves JT (1998) *Langmuir* 120:11977–11985
15. Hosoda N, Kato T (2001) *Chem Mater* 13:688–693
16. Zhang S, Gonsalves KE (1998) *Langmuir* 14:6761–6766
17. Kato T, Suzuki T, Irie T (2000) *Chem Lett* 29:186–187
18. Wada N, Suda S, Kanamura K, Umegaki T (2004) *J Colloid Interf Sci* 279:167–174
19. Kato T, Sugawara A, Hosoda N (2002) *Adv Mater* 14:869–877
20. Jiao Y, Feng Q, Li X (2006) *Mater Sci Eng C* 26:648–652
21. Kitamura M (2000) *J Colloid Interf Sci* 236:318–327
22. Aizenberg J, Lambert G, Weiner S, Addadi L (2002) *J Am Chem Soc* 124:32–39
23. Pieper G, Rehage H, Barthès-Biesel D (1998) *J Colloid Interf Sci* 202:293–300
24. Hacke S (2001) *Brewsterwinkel-Mikroskopie zur Untersuchung der Kristallisation von Calciumcarbonaten an der Modell-Monofilmen an der Grenzfläche Wasser/Luft*. PhD thesis. University of Göttingen, Germany
25. Hacke S, Möbius D (2004) *Colloid Polym Sci* 282:1242–1246
26. Backov R, Lee CM, Khan SR, Mingotaud C, Fanucci GE, Talham DR (2000) *Langmuir* 16:6013–6019
27. Benitez IO, Talham DR (2004) *Langmuir* 20:8287–8293
28. Buijnsters PJJ, Donners JJM, Hill SJ, Heywood BR, Nolte RJM, Zwanenburg B, Sommerdijk NAJM (2001) *Langmuir* 17:3623–3628
29. Heywood BR, Mann S (1994) *Chem Mater* 6:311–318
30. Mann S, Heywood BR, Rajam S, Walker JBA (1991) *J Phys D* 24:154–164
31. Mann S, Archibald DD, Didymus JM, Douglas T, Heywood BR, Meldrum FC, Reeves NJ (1993) *Science* 261:1286–1292
32. Buijnsters PJJ, Donners JJM, Hill SJ, Heywood BR, Nolte RJM, Zwanenburg B, Sommerdijk NAJM (2001) *Langmuir* 17:3623–3628
33. Heywood BR, Mann S (1994) *Chem Mater* 6:311–318
34. Mann S, Heywood BR, Rajam S, Walker JBA (1991) *J Phys D* 24:154–164
35. Mann S, Archibald DD, Didymus JM, Douglas T, Heywood BR, Meldrum FC, Reeves NJ (1993) *Science* 261:1286–1292
36. Cölfen H, Mann S (2003) *Angew Chem Int Edn* 42:2350–2365
37. Moulin P, Roques H (2003) *J Colloid Interf Sci* 261:115–126
38. Ogino T, Suzuki T, Sawada K (1987) *Geochim Cosmochim Acta* 51:2757–2767
39. Olszta MJ, Odom DJ, Douglas EP, Gower LB (2003) *Connect Tissue Res* 44:326–334